Thermal analysis of the cavity facet for an 808 nm semiconductor laser by using near-field scanning optical microscopy

Rao Lan(饶岚)[1, 2], Song Guofeng(宋国峰)[1], and Chen Lianghui(陈良惠)[1, †]

(1 Institute of Semiconductors, Chinese Academy of Sciences, Beijing 100083, China)
(2 School of Electronic Engineering, Beijing University of Posts and Telecommunications, Beijing 100876, China)

Abstract: In order to analyze the thermal characteristics of the cavity facet of a semiconductor laser, a home-built near-field scanning optical microscopy (NSOM) is employed to probe the topography of the facet. By comparing the topographic images of two samples under different DC current injections, we can find that the thermal characteristic is related to its lifetime. We show that it is possible to predict the lifetime of the semiconductor laser diode with non-destructive tests.

Key words: semiconductor laser; NSOM; thermal expansion
DOI: 10.1088/1674-4926/31/10/104007 **EEACC:** 2520

1. Introduction

High power semiconductor lasers have been widely used, e.g., as pumping solid-state lasers, in medical systems and material processing[1]. As the output power increases, the reliability of the high power laser is crucial for practical applications. The laser diode is heated by the high output power and its temperature increases until thermal runoff takes place at the critical temperature. The temperature increase results in a drastic reduction in the device lifetime. Analysis of the thermal characteristic of the semiconductor laser diode is important to investigate the device lifetime. Theoretically, regression models are developed to predict the lifetime of the diode lasers[2]. Experimentally, on the one hand, the device thermal characteristics are related to various parameters such as threshold current, emission wavelength, and junction voltage[3], which are sensitive to the temperature changes in the device. On the other hand, there are several techniques which are potentially helpful for the thermal analysis of laser diode devices, such as micro-Raman spectroscopy[4−6], electroluminescence[7, 8], photoluminescence[9−11], scanning near field infrared radiometry (SNIM)[12, 13], thermo-reflectance (TR)[14−16], and scanning thermal microscopy (SThM)[17, 18]. These techniques have proved to be useful for estimating the temperature of the laser facet. In this paper, we employ a home-built near-field scanning optical microscope (NSOM) to investigate the thermal properties of the laser diode. Compared to the accelerated aging test, the lifetime of the laser diode can be predicted without destruction using this method.

2. Method

In our experiments, we employ the home-built NSOM to image the topography of the front facet of a semiconductor laser diode (LD). When the probe is scanning at the front facet of the LD, the LD is driven with a constant continuous current. The NSOM works in constant gap-width mode to protect the LD's facet. The scanning rate is fixed at 0.302 Hz and the scan area is about $20 \times 20~\mu\text{m}^2$. Figure 1(a) shows the experimental setup diagram we employed, i.e. the Cartesian coordinate system. The x–y plane is the front facet of the laser diode. The x direction is perpendicular to the active layer of the laser diode; the y direction is parallel to the active layer; while the z direction is along the resonant cavity of the laser diode.

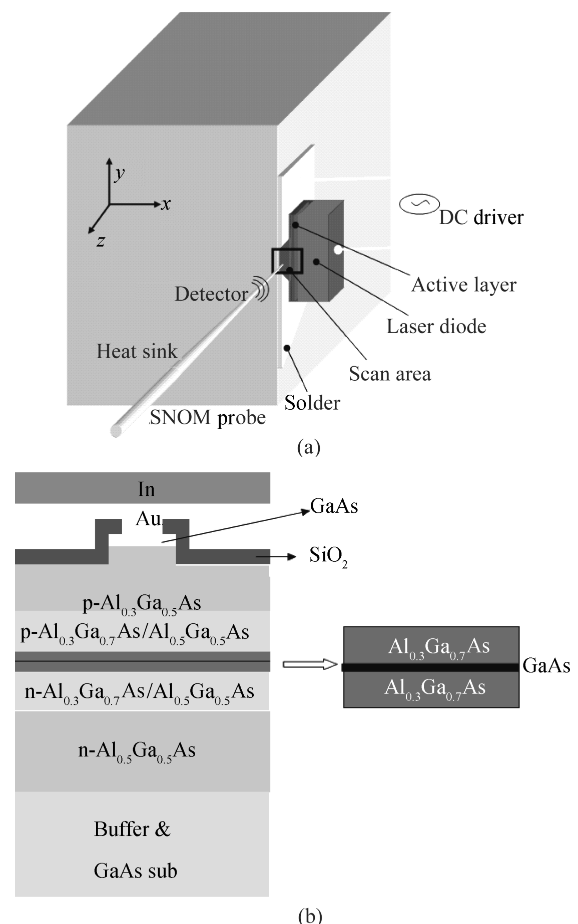

Fig. 1. (a) Experimental diagram. (b) Structure of the laser diode.

† Corresponding author. Email: chenlh@semi.ac.cn
Received 7 April 2010

© 2010 Chinese Institute of Electronics

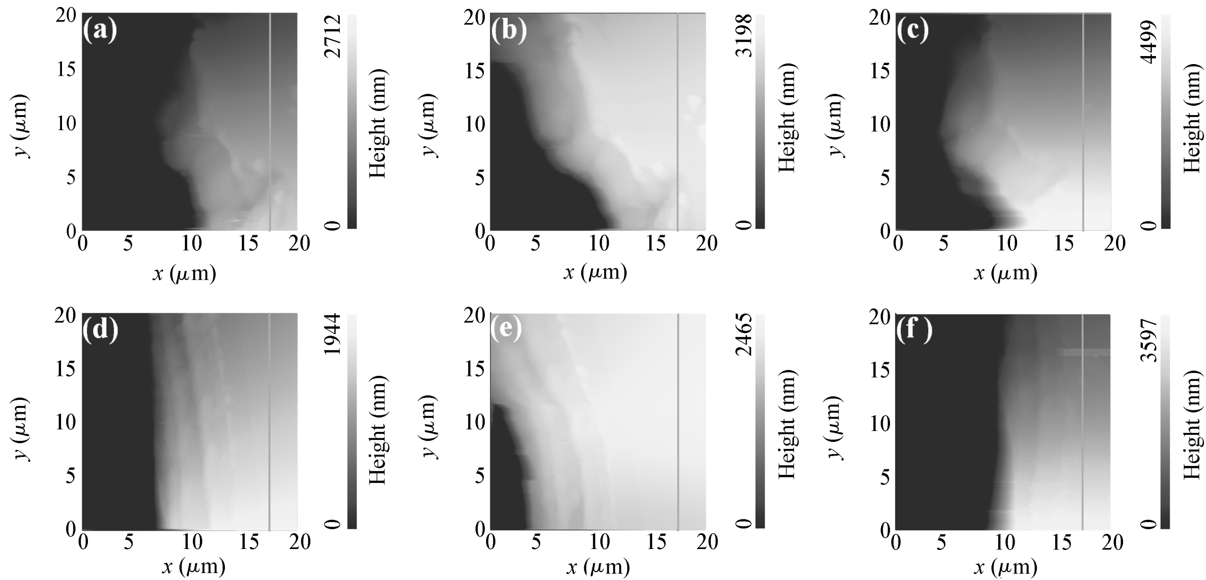

Fig. 2. Topographic images measured by the NSOM. (a)–(c) are the images of LD-A. (a) Original topographic image of the laser face before current injection. (b), (c) First topographic image after the injection current is switched on and off, respectively. (d)–(f) are the corresponding images for LD-B, respectively. The lines in the images are drawn to represent the scan lines for the following analysis.

The LD sample prepared for experiment is fabricated in our lab, and its lasing wavelength is about 808 nm. The structure of the laser diode is shown in Fig. 1(b). It is an AlGaAs broad-area laser diode in which the epitaxial layers are grown on an n-GaAs substrate. The active region consists of an AlGaAs single quantum well (QW) layer between symmetrical AlGaAs waveguide and cladding layers. The laser diode is p-side down mounted on a Cu heat sink. In our experiments, we prepare two laser diode samples with the same process, called laser diode sample A (LD-A) and laser diode sample B (LD-B).

The NSOM is first used to image the topography of the laser diode facet before the LD is driven. Then, we start a new set of scans and obtain topographic images when the LD is driven by a constant continuous current. The active region can be found by comparing the topographic and optical images, because these images are the function of the tip position and obtained at the same time. We scan the laser facet three times and find that there are few changes for the topographic images. We switch off the injection current after the third scan is finished and start a new set of scans simultaneously. The topographic image is same as the original one as long as the scanning time is long enough. Figure 2 shows the topographic images measured by the NSOM. Figures 2(a), 2(b), and 2(c) show topographic images of LD-A measured before, during and after current injection, respectively. Figures 2(b) and 2(c) are the first images when we switch on and off the injection current, respectively. The corresponding images for LD-B are shown in Figs. 2(d), 2(e), and 2(f). In these images, the bright and dark regions correspond to the image of the LD and the heat sink, respectively, because the facet of the laser diode is little higher than that of the heat sink in our experimental samples.

By comparing the topographic images with and without injection current, we can find the influences of the injection current on the topographic images of the laser diode. Changes perpendicular to the active layer (along the x direction) and changes of the height in the images (along the z direction) are obviously observed. The explanation for this is that when the laser diode is operating, one part of the power injected into the LD is converted into emitted light and another part of it is converted into heat which causes thermal expansion due to the rise of LD's temperature.

3. Results

The height changes due to thermal expansion along the z direction. Figures 3(a) and 3(b) show the raw data taken from the topographic images along the scanning lines from the bottom to the top, and the positions of the scanning lines are drawn as shown in Figs. 2(a)–2(f). In Fig. 3(a), the data of A (black), A-up (red) and A-down (green) lines are the raw data taken from Figs. 2(a), 2(b), and 2(c), respectively. The data represent the height along the z direction. By comparing the lines in Fig. 3(a), we can find that the slope of the cross lines are different. The difference is due to thermal expansion of the LD due to the current injection.

In the experiments, the scanning rate is constant. The data are obtained at each tip position step by step. The interval between two pieces of obtained data is the same. The data of the images are measured as a function of tip position. Therefore, the relationship between the scanning time and the tip position is linear.

In order to analyze the main difference between the height changes of LD-A, we numerically subtract A data from A-up data and A-down data, respectively, as shown in Fig. 3(b). The data of the triangle symbol (new A-up) are the original A-up data with the A data numerically subtracted. The data of the square symbol (new A-down) are deduced from the original A-down data. That is, the data represent the height difference after the injection current is switched on and off, respectively. In Fig. 3(b), the red line is the averaging line for the new A-up data. After the injection current is switched on, the temperature of the LD increases. As a consequence, thermal expansion

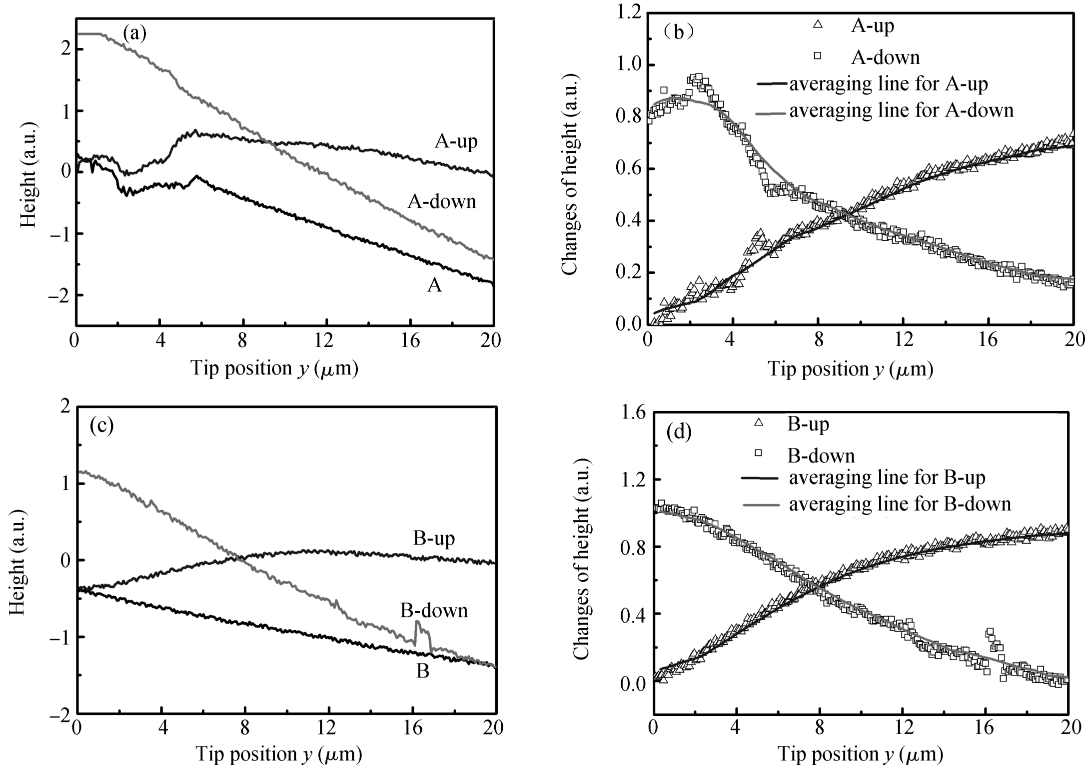

Fig. 3. Results deduced from raw data (Fig. 2). (a) Raw data of LD-A: A, A-up and A-down obtained from the images of Figs. 2(a), 2(b), and 2(c), respectively. (b) Difference of the height abstracted from raw data in Fig. 3(a). (c), (d) Corresponding results for laser sample B, respectively.

occurs. The length of the laser resonant cavity becomes longer than before. The slope of the red line is positive. In contrast, the slope of the green line in Fig. 3(b) which is the average line for the new A-down data is negative. The green line represents the height changes when the injection current is switched off. The LD's temperature is little higher than that of heat sink when the LD is working. As the injection current is turned off, the thermal equilibrium of the LD is destroyed. The LD's temperature decreases. The length of the LD's resonant cavity becomes shorter.

A similar thing occurs as we deal with the topographic images of LD-B with the same method. Figures 3(c) and 3(d) are the corresponding results, respectively. Figure 3(c) shows the raw data of B (black), B-up (red) and B-down (green) obtained from Figs. 2(d), 2(e), and 2(f), respectively. Figure 3(d) shows the relationship between the height changes caused by the injection current along the y scanning direction.

4. Discussions

There are three mechanisms for the heat energy exchange between device and environment: conduction, convection and radiation. In the steady state, the power generated by a device is balanced by the power removed from the device and we can write it as:

$$Q_{\text{gen}} = Q_{\text{cond}} + Q_{\text{conv}} + Q_{\text{rad}}, \tag{1}$$

where Q_{gen} is the total heat power generated by the injection current, Q_{cond} is the conduction power, Q_{conv} is the convection power, and Q_{rad} is the radiation power. In our experiments, the injection current (I) is fixed at 100 mA, which is less than the threshold currents of the laser samples. That is, the laser diode is not lasing, just working in fluorescence. The optical power is a small part of the input power. Here, we assume that the input power of sample laser A is same as that of sample laser B when we add the injection current to drive the laser diodes and Q_{gen} ($\approx IV$) is converted into heat.

The temperature rise will cause thermal expansion. The local expansion signal l can be written as $l = \alpha L \Delta T$, where α is the local thermal expansion-coefficient, L is the local sample height and ΔT is the local temperature rise. Since the local height α is already contained in the topography, the expansion signal can be used to obtain local material characteristics through α or temperature rise through ΔT. Here, the local thermal expansion-coefficient is assumed as a constant. Therefore, the local temperature change (ΔT) is proportional to the local expansion signal l which is the change of the height of the sample laser (along the z direction).

In our experiments, we compare the thermal characteristics of the two laser diodes to understand temperature changes caused by the current injection. As mentioned above, the scan rate is constant, at 0.302 Hz, in our experiment. The tip position is proportional to the scan time. Since we start a new scan when the injection current is switched on simultaneously, the scan time represents the injection time. In this condition, the relationship between the temperature changes of the laser diode and the scan time can be deduced.

Figure 4(a) gives the normalization of the A-up (circle symbol) data and B-up (triangle symbol) data as a function of the current injection time. L1 (black line) and L2 (red line) are fit-

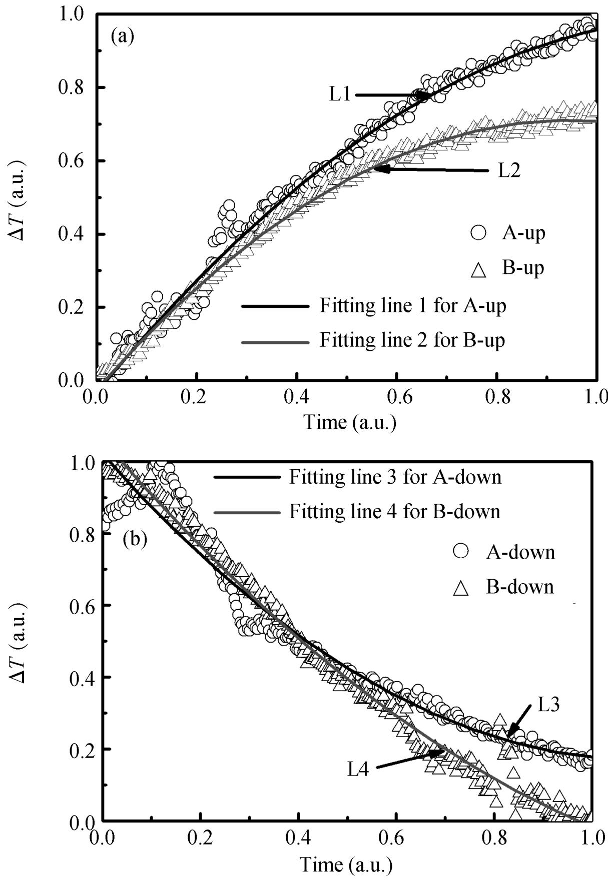

Fig. 4. Comparison of the results of lasers A and B. (a) shows the result as the current is injected. L1 (black) is the fitting line for the A-up data. L2 (red) is the fitting line for the B-up data. (b) shows the result as the injection current is switched off. L3 (black) is the fitting line for the A-down data. L4 is the fitting line for the B-down data.

ting lines for the new A-up data and new B-up data, respectively. As the same power is added to the laser diode, the temperature change of LD-A is faster than that of LD-B as time goes on, and the thermal balance temperature of LD-B is lower than that of LD-A.

Figure 4(b) shows the normalized results of the new A-down (blue circle symbol) data and new B-down (green triangle symbol) data. L3 (black line) and L4 (red line) are the fitting lines. L3 and L4 decrease as the time increases. This means that, when the injection current is switched off, the temperature of the laser diode will decrease. The absolute value of the slope of L4 is bigger than that of L3. The explanation for this is that the rate of thermal exchange with the environment of LD-B is faster than that of LD-A. Above all, the thermal property of LD-B is better than that of LD-A.

An aging test has been done to understand the relationship between the thermal characteristics and the lifetime of the laser diode. The aging testing injection current is 1 A. Figure 5 shows the I–V and I–P curve at 0 h (at the beginning of the test), 40 h (after lightening for 40 h, and 146 h (after lightening for 146 h). After 146 h, LD-A is dead while the lifetime of LD-B is more than 441 h. We find that the lifetime of LD-B is longer than that of LD-A. As we show above, the thermal property of LD-B is better than that of LD-A. When we add the same injection current to drive the laser diode, the temperature

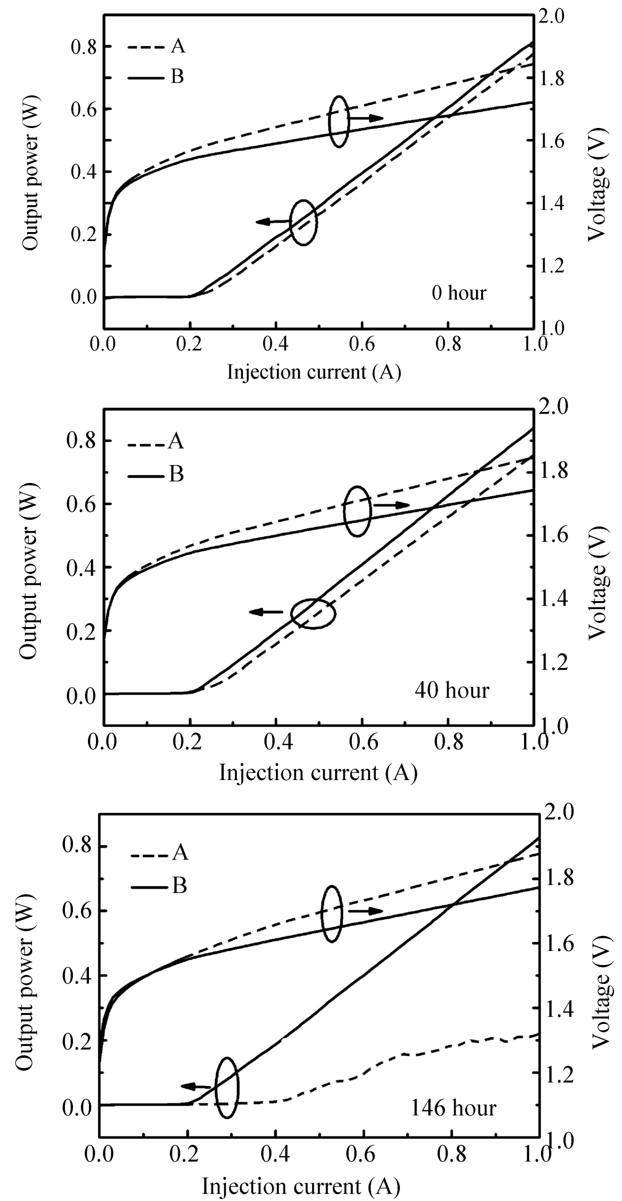

Fig. 5. Aging test results. 0 hour is at the beginning of the test. 40 hour is measured when the laser diode has operated for 40 h. 146 hour is measured when the laser diode has operated for 146 h.

of LD-A will be higher than that of LD-B, the temperature rise will accelerate aging, and the lifetime of the laser is shortened. The relationship between the thermal property detected in this method and the lifetime of the laser diode will be studied in future.

5. Conclusions

In conclusion, we present a new method to estimate the thermal properties of an 808 nm semiconductor laser by NSOM. We describe the experimental set-up and the experimental process in detail. Topographic images of the facet of the LDs are measured before, during and after DC current injection. By comparing the topographic images, we can deduce the thermal characteristics of the LD. As we all know, the better the thermal property, the longer the lifetime of the semiconductor laser. Thus, the method introduced in this paper may

provide a way to predict the lifetime of a semiconductor laser diode without destruction.

References

[1] Walker C L, Bryce A C, Marsh J H. Improved catastrophic optical damage level from laser with nonabsorbing mirrors. IEEE Photonics Technol Lett, 2002, 14(10): 1394

[2] Li Y. Lifetime prediction of diode lasers with different aging behaviors. SPIE, 2007, 6485: 648519

[3] Kirkup L, Kalceff W, McCredie G. Effect of injection current on the repeatability of laser diode junction voltage–temperature measurements. J Appl Phys, 2007, 101: 023118

[4] Tien T Q, Weik F, Tomm J W, et al. Thermal properties and degradation behavior of red-emitting high-power diode lasers. Appl Phys Lett, 2006, 89: 181112

[5] Sanayeh M B, Brick P, Schmid W, et al. Temperature–power dependence of catastrophic optical damage in AlGaInP laser diodes. Appl Phys Lett, 2007, 91: 041115

[6] Ziegler M, Talalaev V, Tomm J W, et al. Surface recombination and facet heating in high-power diode lasers. Appl Phys Lett, 2008, 92: 203506

[7] Rossetti M, Smeeton T M, Tan W S, et al. Degradation of InGaN/GaN laser diodes analyzed by microphotoluminescence and microelectroluminescence mappings. Appl Phys Lett, 2008, 92: 151110

[8] Bull S, Andrianov A V, Harrison I, et al. A spectroscopically resolved photo- and electroluminescence microscopy technique for the study of high-power and high-brightness laser diodes. IEEE Trans Instrum Meas, 2005, 54(3): 1079

[9] Rommel J M, Gavrilovic P, Dabkowski F P. Photoluminescence measurement of the facet temperature of 1 W gain-guided AlGaAs/GaAs laser diodes. J Appl Phys, 1996, 80(11): 6547

[10] Chavan A, Radionova R, Charache G W, et al. Comparison of facet temperature and degradation of unpumped and passivated facets of Al-free 940-nm lasers using photoluminescence. IEEE J Quantum Electron, 2005, 41(5): 630

[11] Sanayeh M B, Jaeger A, Schmid W, et al. Thermal relaxation time and heat distribution in pulsed InGaAs quantum dot lasers. Appl Phys Lett, 2006, 89: 101111

[12] Sade S, Nagli L, Katzir A. Scanning near field infrared radiometry for thermal imaging of infrared emitters with subwavelength resolution. Appl Phys Lett, 2005, 87: 101109

[13] Ziegler M, Tomm J W, Elsaesser T, et al. Real-time thermal imaging of catastrophic optical damage in red-emitting high-power diode lasers. Appl Phys Lett, 2008, 92: 103514

[14] Luerssen D, Hudgings J A, Mayer P M, et al. Nanoscale thermoreflectance with 10 mK temperature resolution using stochastic resonance. 21st IEEE Semi-Therm Symposium, 2005, 3: 253

[15] Ochalski T J, Pierśicńska D, Pierściński K, et al. Complementary thermoreflectance and micro-Raman analysis of facet temperatures of diode lasers. Appl Phys Lett, 2006, 89: 071104

[16] Dilhaire S, Grauby S, Claeys W. Thermoreflectance calibration procedure on a laser diode: application to catastrophic optical facet damage analysis. IEEE Electron Device Lett, 2005, 26(7): 461

[17] Majumdar A, Luo K, Shi Z, et al. Scanning thermal microscopy at nanometer scales: a new frontier in experimental heat transfer. Experimental Heat Transfer, 1996, 9(2): 83

[18] Kim K, Chung J, Won J, et al. Quantitative scanning thermal microscopy using double scan technique. Appl Phys Lett, 2008, 93: 203115